

Magnetization plateau and incommensurate spin modulation in $\text{Ca}_3\text{Co}_2\text{O}_6$

Yang Zhao, Shou-Shu Gong, Wei Li, Gang Su*

College of Physical Sciences, Graduate University of Chinese Academy of Sciences,
P. O. Box 4588, Beijing 100049, People's Republic of China

The magnetic properties of a trigonal prism unit of the spin-2 frustrated compound $\text{Ca}_3\text{Co}_2\text{O}_6$ are studied by means of the density-matrix renormalization group method. A magnetization plateau at $m_s/3$ (m_s is the saturation magnetization) with ferrimagnetic structure is observed. By fitting the experimental data of magnetic curve, an estimation of the couplings gives $J_1 = -26.84\text{K}$, $J_2 = 0.39\text{K}$, and $J_3 = 0.52\text{K}$. The local magnetic moments are unveiled to exhibit an incommensurate sinusoidally modulation along the three chains of the trigonal prism, which gives a strong theoretical support to the experimentally observed incommensurate partially disordered antiferromagnetic state for $\text{Ca}_3\text{Co}_2\text{O}_6$. The present result suggests that the modulation indeed originates from the competition of antiferromagnetic and ferromagnetic couplings.

Frustrated quantum magnets have been extensively studied owing to their exotic properties [2]. Among others, the first experimental realization of ferromagnetic (FM) chains coupled with antiferromagnetic (AFM) interactions in a triangular plane in the spin frustrated chain compound $\text{Ca}_3\text{Co}_2\text{O}_6$ has attracted much attention in the last decade [3–5]. $\text{Ca}_3\text{Co}_2\text{O}_6$ consists of spin chains with alternating face-sharing octahedral (Co I) and trigonal prismatic (Co II) CoO_6 polyhedra along the c axis, and arranged in a triangular lattice in the ab plane [3], as shown schematically in Fig. 1(a). The Co^{3+} ions on the Co I and Co II sites have low-spin ($S=0$) and high-spin ($S=2$) states, respectively [6]. Within the chains, direct Co-Co overlap leads to a strong FM intrachain interaction J_1 (about 25K) [7]. For the AFM interchain super-superexchange interactions J_2 and J_3 , as the overlap of the O $2p$ orbital is very small, J_2 is weaker than J_3 [7].

A number of techniques (x-ray [8, 9], neutron scattering [10], NMR [6], calorimetry [11], and μSR [12], etc.) have been used to study this intriguing compound in different aspects, such as the nature of the order at different temperatures, the magnetization process under various conditions, and so on. It was found that the compound has two transition temperatures $T_{c1} \simeq 25\text{K}$ and $T_{c2} \simeq 7\text{K}$, between which the magnetization curve has a $m_s/3$ plateau (m_s is the saturation magnetization) [3]. Below T_{c2} , the magnetization shows a multistep structure and the hysteresis, which was suggested in a spin freezing state [3, 4], and appears still under debate. Another intriguing issue is the magnetic state between T_{c1} and T_{c2} in absence of a magnetic field. Owing to the spin frustration, two possible magnetic structures were proposed: (1) a ferrimagnetic (FI) structure, with two third of spins up and one third spins down; (2) a partially disordered antiferromagnetic (PDA) structure, with one third spins up, one third spins down, and one third spins incoherent.

Recently, the zero-field magnetic state of $\text{Ca}_3\text{Co}_2\text{O}_6$ between T_{c1} and T_{c2} has been shown to be a sinusoidally modulated incommensurate PDA (iPDA) state with a modulation of very long periodicity ($\sim 1000\text{\AA}$) along the chain direction by resonant X-ray scattering [9, 13] and neutron diffraction [14] measurements. Such a magnetic structure cannot be explained in a simple two-dimensional (2D) triangular Ising model [15], in contrast to some previous works. Therefore, to understand the iPDA state, the trigonal prism unit of $\text{Ca}_3\text{Co}_2\text{O}_6$ includ-

ing all possible Heisenberg interactions should be considered [14, 16]. In the trigonal prism, the AFM interchain couplings J_2 and J_3 follow helical paths and connect the Co II ($S=2$) sites in adjacent chains [Fig. 1(a)]. The competition between the AFM and FM interactions was argued to be responsible for the modulation [14, 16]. The emergence of the iPDA state was suggested to be related to the trigonal prism unit [16]. However, a direct theoretical analysis of the iPDA state in the trigonal prism unit of $\text{Ca}_3\text{Co}_2\text{O}_6$ is still absent.

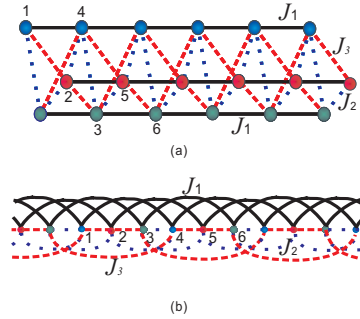


FIG. 1: (Color online) (a) Schematic structure of the trigonal prism unit of $\text{Ca}_3\text{Co}_2\text{O}_6$, J_1 (black lines) FM; J_2 (blue dotted lines) AFM; J_3 (red dashed lines) AFM. Co II ($S=2$) sites in different chains are colored differently. (b) Sketch of the equivalent $S=2$ spin chain model [Eq. (1)].

In this paper, by means of the density-matrix renormalization group (DMRG) method we shall study the magnetic properties of the $S=2$ spin chain model with the trigonal prism unit under various circumstances, and fit the experimental result of magnetization curve of $\text{Ca}_3\text{Co}_2\text{O}_6$ to estimate the three different couplings J_1 , J_2 and J_3 . The origin of the iPDA state in $\text{Ca}_3\text{Co}_2\text{O}_6$ will also be addressed. Our results show that the system exhibits a $m_s/3$ magnetization plateau with a FI structure, and a very good fitting to the experimental data is obtained, with the theoretical fitting values in well agreement with those obtained by other experimental means. The incommensurate sinusoidally modulated structure with a long period along the chain direction is observed in the local magnetic moments in the present model, which may shed light on the origin of the iPDA state in the compound $\text{Ca}_3\text{Co}_2\text{O}_6$.

The trigonal prism unit of $\text{Ca}_3\text{Co}_2\text{O}_6$ [Fig. 1(a)] can be equivalently expanded to a $S=2$ Heisenberg spin chain with

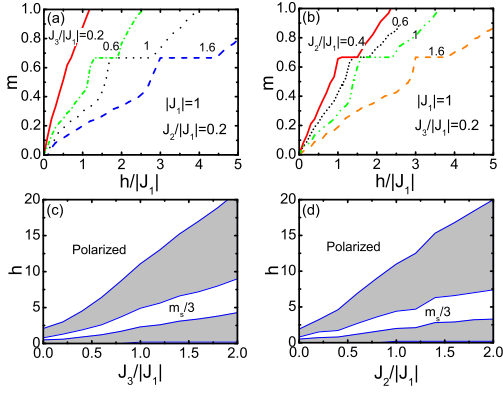


FIG. 2: (Color online) Magnetization curves of spin-2 trigonal prism chain with (a) $J_2/|J_1|=0.2$ for different J_3 , and (b) $J_3/|J_1|=0.2$ for different J_2 . Magnetic phase diagrams in the $h - J_{2,3}$ plane of the $S=2$ trigonal prism chain under interest for (c) $J_2/|J_1|=0.2$, and (d) $J_3/|J_1|=0.2$.

nearest neighbor, next, next next, and next next next nearest neighbor interactions, as illustrated in Fig. 1(b). The Hamiltonian under interest is given by

$$\begin{aligned}
 H = & \sum_{i=1}^{L/3} [J_1(\mathbf{S}_{3i-2} \cdot \mathbf{S}_{3i+1} + \mathbf{S}_{3i-1} \cdot \mathbf{S}_{3i+2} + \mathbf{S}_{3i} \cdot \mathbf{S}_{3i+3}) \\
 & + J_2(\mathbf{S}_{3i-1} \cdot \mathbf{S}_{3i+1} + \mathbf{S}_{3i} \cdot \mathbf{S}_{3i+1} + \mathbf{S}_{3i} \cdot \mathbf{S}_{3i+2}) \\
 & + J_3(\mathbf{S}_{3i-2} \cdot \mathbf{S}_{3i-1} + \mathbf{S}_{3i-1} \cdot \mathbf{S}_{3i} + \mathbf{S}_{3i-3} \cdot \mathbf{S}_{3i+1})] \\
 & - h \sum_{j=1}^{L/3} S_j^z, \quad (1)
 \end{aligned}$$

where \mathbf{S}_j is the $S=2$ spin operator at the j -th site, L is the total number of spins in the trigonal prism, $J_1 < 0$ ($J_{2,3} > 0$) is the FM (AFM) interaction, and h is the magnetic field applied along the chain direction. For convenience, we take $g\mu_B=1$. During the DMRG [17] iteration, the length of the chain is taken at least 90, the optimal states are kept 120, and the truncation error is less than 10^{-5} .

Figs. 2(a) and (b) show the DMRG results of the magnetization curve of the $S=2$ trigonal prism spin chain system for different couplings. It can be seen that under proper couplings, the system has a $m_s/3$ magnetization plateau that is consistent with the necessary condition [18] $n(S - m) = \text{integer}$ for the appearance of magnetization plateau in Heisenberg quantum antiferromagnets, where n is the period of ground state, S is the magnitude of spin, and m is the magnetization per site. For the present system, $n=3$. In the plateau state, the local magnetic moments are found to have the same value in each chain of the trigonal prism, arranged in a FI structure, namely $(-2, 2, 2)$, in agreement with the experimental observation [3]. The width of the plateau increases with increasing AFM interactions J_2 and J_3 , and decreases with increasing FM coupling $|J_1|$, which are consistent with the behaviors of magnetization plateau observed in other systems [19]. Through massive calculations, the magnetic phase diagrams in the $h - J_2(J_3)$ plane can be obtained by observ-

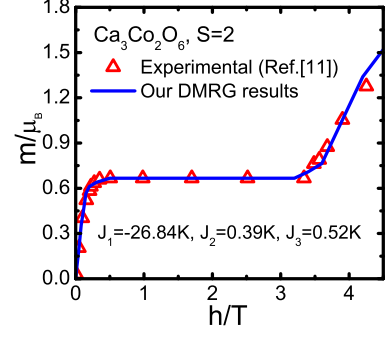


FIG. 3: (Color online) The experimental data of magnetization curve for $\text{Ca}_3\text{Co}_2\text{O}_6$ at $T=10\text{K}$ from Ref. 12 are fitted with the DMRG results, giving $J_1=-26.84\text{K}$, $J_2=0.39\text{K}$ and $J_3=0.52\text{K}$. In the calculation, the number of Co sites is chosen as 180.

ing the critical and saturation magnetic fields of magnetization curves under different couplings, as depicted in Figs. 2(c) and (d). It appears that the region for the appearance of $m_s/3$ magnetization plateau is narrow.

The $m_s/3$ magnetization plateau of the trigonal prism chain compound $\text{Ca}_3\text{Co}_2\text{O}_6$ has been already observed experimentally [12]. To fit the experimental data, we make a lot of DMRG calculations [21]. The fitting results for the data of $T=10\text{K}$ from Ref. 12 are presented in Fig. 3, which shows a good agreement, giving $J_1=-26.84\text{K}$, $J_2=0.39\text{K}$, and $J_3=0.52\text{K}$. The so-obtained J_1 is very close to 25K estimated from the experimental study [3] and first-principle calculations [7] of $\text{Ca}_3\text{Co}_2\text{O}_6$, and $J_3/J_1 \simeq -0.019$ is also consistent with the value -0.018 obtained in Ref. 16 within a classical treatment. Below the plateau, as shown in Fig. 3, the magnetization curve increases very sharply as indicated by a cusp observed experimentally [20] in the magnetic susceptibility, which was once regarded as a feature of FI state of $\text{Ca}_3\text{Co}_2\text{O}_6$ between T_{c1} and T_{c2} . Our DMRG results indicate that the iPDA state can also give rise to a similar behavior below the magnetization plateau.

Now let us look at the incommensurate magnetic modulation observed in $\text{Ca}_3\text{Co}_2\text{O}_6$ through the trigonal prism spin chain model [Eq. (1)]. For this purpose, the magnetic moments are calculated. Figure 4 presents the DMRG result of local magnetic moment $\langle S_j^z \rangle$ for $J_1:J_2:J_3=-1:0.3:0.4$ as an example. To see clearly the magnetic modulation, $\langle S_{3j}^z \rangle$, $\langle S_{3j-1}^z \rangle$ and $\langle S_{3j-2}^z \rangle$, which correspond to the three chains of the trigonal prism in Fig. 1(a), are studied, respectively. It is evident that the spatial dependence of $\langle S_j^z \rangle$ for the three chains along the c axis exhibits modulations sinusoidally around 0.986 ($\langle S_{3j}^z \rangle$), 0.414 ($\langle S_{3j-1}^z \rangle$), and -1.4 ($\langle S_{3j-2}^z \rangle$), indicating that the state is neither FI nor PDA, but an iPDA, thereby supporting the recent experimental observations [9, 13, 14]. During the DMRG calculations, the systems with various chain lengths are compared. It is found that the expectation value of each local magnetic moment $\langle S_j^z \rangle$ is almost independent of the system size, indicating that the modulation is not a finite-size effect. In Fig. 4, we show the case with 120

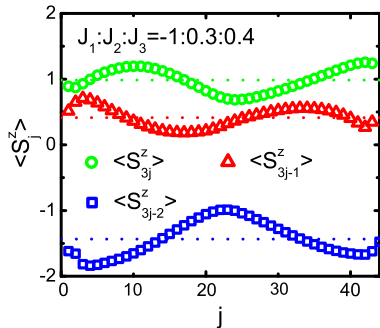


FIG. 4: (Color online) The spatial dependence of the local magnetic moments $\langle S_j^z \rangle$ of the $S=2$ trigonal prism spin chain model for $J_1:J_2:J_3=-1:0.3:0.4$.

sites (40 unit cells) of the $S=2$ spin chain [Eq. (1)] that gives the period of modulation about 36 unit cells, showing that the system can have a magnetic modulation with a long period. Besides, we have also uncovered the less $|J_1|$ ($|J_1| > J_{2,3}$), the shorter the modulation period. When J_2 or J_3 is set zero and $|J_1|$ dominates, the similar magnetic modulations are also seen. In a general case with $|J_1| > J_{2,3}$, the period of modulation is observed to decrease with increasing AFM interactions $J_{2,3}$ and increase with increasing FM coupling $|J_1|$. These evidences show that the modulation indeed originates from the competition between the FM and AFM interactions.

It was argued that the magnetic modulation in $\text{Ca}_3\text{Co}_2\text{O}_6$ may be caused by both the single-ion anisotropy and the competition of couplings [14]. To clarify this point, we consider the effect of single-ion anisotropy $-D \sum_i (S_i^z)^2$ ($D > 0$) on

the magnetic properties of the spin-2 Heisenberg complex chain system [Eq. (1)]. The results show that the single-ion anisotropy weakens the modulation and prolongs the modulation period. For instance, when $D=0.2$, the period exceeds 50 unit cells. With further increasing D , the modulation vanishes and the local magnetic moments in different chains form a FI structure, i.e., $(-2, 2, 2)$ when $D \geq 0.4$. When we replace J_1 terms in Eq. (1) along the three chains as Ising couplings ($J_1 > J_{2,3}$), we find no modulation for the magnetic moments, implying that the 2D triangular Ising treatment cannot describe the observed iPDA state below the plateau.

In summary, the magnetic properties of the $S=2$ trigonal prism unit of $\text{Ca}_3\text{Co}_2\text{O}_6$ are studied by means of the DMRG method. The $m_s/3$ magnetization plateau with a FI structure is observed, which is consistent with the experimental observation. The phase diagrams in the $h - J_{2,3}$ plane are obtained. The experimental data of magnetic curve of $\text{Ca}_3\text{Co}_2\text{O}_6$ are nicely fitted to the DMRG results, giving an estimation of the interactions $J_1 = -26.84\text{K}$, $J_2 = 0.39\text{K}$, and $J_3 = 0.52\text{K}$, in agreement with the previous experimental measurement. The iPDA state with a long period observed experimentally is supported by the calculated incommensurate sinusoidally modulated magnetic moments in the trigonal prism unit of $\text{Ca}_3\text{Co}_2\text{O}_6$. The effects of single-ion anisotropy and Ising limit are also discussed. Our calculation gives a strong support to the proposal that the iPDA state originates from the frustration due to the competition between the intrachain FM interaction and the interchain AFM couplings, and indicates the crucial role of the trigonal prism structure in understanding the iPDA state of $\text{Ca}_3\text{Co}_2\text{O}_6$.

This work is supported in part by the NSFC (Grant Nos. 10625419, 10934008, 90922033), the MOST of China (Grant No. 2006CB601102) and the Chinese Academy of Sciences.

- [1] *Corresponding author. E-mail: gsu@gucas.ac.cn
- [2] H. T. Diep, *Frustrated Spin Systems* (World Scientific Publishing Co. Pte. Ltd., Singapore, 2004).
- [3] H. Fjellvåg, E. Gulbrandsen, S. Asland, A. Olsen, and B. C. Hauback, *J. Solid State Chem.* **124**, 190 (1996); H. Kageyama, K. Yoshimura, K. Kosuge, M. Azuma, M. Takano, H. Mitamura, and T. Goto, *J. Phys. Soc. Jpn.* **66**, 3996 (1997).
- [4] A. Maignan, C. Michel, AC Masset, C. Martin, and B. Raveau, *Eur. Phys. J. B* **15**, 657 (2000).
- [5] V. Hardy, M. R. Lees, O. A. Petrenko, D. McK. Paul, D. Flahaut, S. Hébert, and A. Maignan, *Phys. Rev. B* **70**, 064424 (2004).
- [6] E. V. Sampathkumaran, N. Fujiwara, S. Rayaprol, P. K. Madhu, and Y. Uwatoko, *Phys. Rev. B* **70**, 014437 (2004).
- [7] R. Frésard, C. Laschinger, T. Kopp, and V. Eyert, *Phys. Rev. B* **69**, 140405 (R) (2004).
- [8] K. Takubo, T. Mizokawa, S. Hirata, J.-Y. Son, A. Fujimori, D. Topwal, D. D. Sarma, S. Rayaprol, and E.-V. Sampathkumaran, *Phys. Rev. B* **71**, 073406 (2005); T. Burnus, Z. Hu, M. W. Haverkort, J. C. Cezar, D. Flahaut, V. Hardy, A. Maignan, N. B. Brookes, A. Tanaka, H. H. Hsieh, H.-J. Lin, C. T. Chen, and L. H. Tjeng, *Phys. Rev. B* **74**, 245111 (2006).
- [9] S. Agrestini, C. Mazzoli, A. Bombardi, and M. R. Lees, *Phys. Rev. B* **77**, 140403 (R) (2008).
- [10] S. Aasland, H. Fjellvåg, B. Hauback, *Solid State Commun.* **101**, 187 (1997); O. A. Petrenko, OA Petrenko, J. Wooldridge, M. R. Lees, P. Manuel, and V. Hardy, *Eur. Phys. J. B* **47**, 79 (2005).
- [11] V. Hardy, S. Lambert, M. R. Lees, and D. McK. Paul, *Phys. Rev. B* **68**, 014424 (2003).
- [12] S. Takeshita, T. Gokoa, J. Araia, and K. Nishiyama, *J. Phys. Chem. Solids* **68**, 2174 (2007).
- [13] C. Mazzoli, A. Bombardi, S. Agrestini, M. R. Lees, *Physica B* **404**, 3042 (2009).
- [14] S. Agrestini, L. C. Chapon, A. Daoud-Aladine, J. Schefer, A. Gukasov, C. Mazzoli, M. R. Lees, and O. A. Petrenko, *Phys. Rev. Lett.* **101**, 097207 (2008).
- [15] Y. B. Kudasov, *Phys. Rev. Lett.* **96**, 027212 (2006); X. Yao, S. Dong, H. Yu, and J. Liu, *Phys. Rev. B* **74**, 134421 (2006).
- [16] L. C. Chapon, *Phys. Rev. B* **80**, 172405 (2009).
- [17] S. R. White, *Phys. Rev. Lett.* **69**, 2863 (1992); S. R. White, *Phys. Rev. B* **48**, 10345 (1993); U. Schollwöck, *Rev. Mod. Phys.* **77**, 259 (2005).
- [18] M. Oshikawa, M. Yamanaka, and I. Affleck, *Phys. Rev. Lett.* **78**, 1984 (1997).
- [19] B. Gu, Gang Su, *J. Phys.:Condens. Matter* **17**, 6081 (2005); *Phys. Rev. B* **75**, 174437 (2007); B. Gu, Gang Su, and Song Gao, *Phys. Rev. B* **73**, 134427 (2006);
- [20] B. Martinez, V. Laukhin, M. Hernando, J. Fontcuberta, M. Parra, and J. M. Gonzalez-Calbet, *Phys. Rev. B* **64**, 012417 (2001).
- [21] As the present model has a high spin state ($S=2$) and contains complex interactions, a direct finite-temperature DMRG calculation is almost impermissible. Therefore, we perform the

DMRG calculations to fit the magnetization curve at $T=10\text{K}$.